Luminal fructose inhibits rat intestinal sodium-phosphate cotransporter gene expression and phosphate uptake[1–5]

Séverine Kirchner, Anjali Muduli, Donatella Casirola, Kannitha Prum, Véronique Douard, and Ronaldo P Ferraris

ABSTRACT

Background: While searching by microarray for sugar-responsive genes, we inadvertently discovered that sodium-phosphate cotransporter 2B (NaPi-2b) mRNA concentrations were much lower in fructose-perfused than in glucose-perfused intestines of neonatal rats. Changes in NaPi-2b mRNA abundance by sugars were accompanied by similar changes in NaPi-2b protein abundance and in rates of inorganic phosphate (Pi) uptake.

Objective: We tested the hypothesis that luminal fructose regulates NaPi-2b.

Design: We perfused into the intestine fructose, glucose, and non-metabolizable or poorly transported glucose analogs as well as phlorizin.

Results: NaPi-2b mRNA concentrations and Pi uptake rates in fructose-perfused intestines were $\approx$30% of those in glucose and its analogs. NaPi-2b inhibition by fructose is specific because the mRNA abundance and activity of the fructose transporter GLUT5 (glucose transporter 5) increased with fructose perfusion, whereas those of other transporters were independent of the perfusate. Plasma Pi after 4 h of perfusion was independent of the perfusate, probably because normal kidneys can maintain normophosphatemia. Inhibiting glucose-6-phosphatase, another fructose-responsive gene, with tungstate or vanadate nonspecifically inhibited NaPi-2b mRNA expression and Pi uptake in both glucose- or fructose-perfused intestines. The AMP kinase (AMPK)–activator AICAR (5-aminoimidazole-4-carboxamide-1-β-D-ribofuranoside) enhanced and the fatty acid synthase–AMPK inhibitor C75 (3-carboxy-4-octyl-2-methylene-butyrolactone *trans*-4-carboxy-5-octyl-3-methylenebutyrolactone) prevented fructose inhibition of NaPi-2b but had no effect on expression of other transporters. NaPi-2b expression decreased markedly with age and was inhibited by fructose in all age groups.

Conclusions: Energy levels in enterocytes may play a role in NaPi-2b inhibition by luminal fructose. Consumption of fructose that supplies $\approx$10% of caloric intake by Americans clearly affects absorption of Pi and may promote Pi homeostasis in patients with impaired renal function. *Am J Clin Nutr* 2008;87:1028–38.

INTRODUCTION

Inorganic phosphate (Pi) is required for bone mineralization and for many biological processes involving intermediary metabolism and energy transfer. Serum Pi concentrations are primarily regulated by 4 hormones: calcitriol or 1,25 dihydroxyvitamin D, parathyroid hormone, calcitonin, and phosphatonins (1, 2). Under normal conditions, the kidney excretes the equivalent amounts of Pi absorbed by the small intestine, and, in adults, there is no net accumulation of Pi in the body. The kidney responds rapidly to alterations in concentrations of dietary Pi and of hormones regulating Pi (3, 4); hence, it is the major regulator of Pi homeostasis. When renal function is compromised as in end-stage renal disease (ESRD), serum Pi increases inevitably because dialysis removes only 70% of Pi absorbed by the intestine (5).

The uptake of Pi is mediated by sodium-phosphate cotransporters (NaPi) that are located at the apical border of the intestinal and proximal tubule cells (1, 6). Chronic consumption of low amounts of dietary phosphorus increases NaPi-2b mRNA and transporter abundances in the apical membrane of small intestinal cells, resulting in increases in Pi uptake (7). The effect of dietary phosphorus on intestinal Pi transport seems mediated by calcitriol (1), although some evidence indicates that dietary phosphorus either directly affects intestinal Pi transport or uses a signal that is independent of vitamin D (3). NaPi-2b is also regulated by systemic nicotinamide (8), estrogen (9), and the phosphatonin FGF23 (2).

Because of dramatic increases in consumption of soft drinks and fruit juices, per capita consumption of fructose has increased by 10 times in 30 y to almost 60 g fructose/d (10, 11). Paralleling this increase in fructose consumption is an alarming increase in incidence of obesity and type 2 diabetes (10). What makes this correlation disturbing is that per capita fructose consumption in very young children has increased faster than that of the general population and in the 1980s was already $\approx$30–40 g fructose/d, representing 10% of their energy intake (11). Thus, fructose is already an important component in the American diet, but there

are few studies on physiologic effects of excessive fructose consumption.

Intestinal nutrient transporters are specifically regulated by their substrates (12). For example, increases in dietary fructose stimulate the transcription of the intestinal fructose transporter GLUT5, thereby increasing fructose transport (13). While searching for glucose- and fructose-responsive genes in the neonatal rat small intestine with microarray, we discovered that there were dramatic differences in NaPi-2b mRNA concentrations between glucose- and fructose-perfused intestines (14). Studies on regulation of intestinal Pi transport and metabolism have become highly relevant to efforts in alleviating the hyperphosphatemia of ESRD, because the intestinal pathway is so critical to regulating Pi homeostasis when the kidneys have failed. Because Pi uptake across the apical membrane is the rate-limiting step in transepithelial Pi transport, NaPi-2b represents an ideal target for regulation (15).

In this study, we tested the hypothesis that NaPi-2b gene expression and activity are regulated by sugars, determined whether luminal fructose or glucose or both were the signal modulating NaPi-2b, evaluated the contribution of glucose-6-phosphatase (G6Pase) and of AMP-activated protein kinase (AMPK) to sugar-mediated regulation of NaPi-2b, and then determined NaPi-2b regulation during development.

MATERIALS AND METHODS

Animals

Adult male and female Sprague-Dawley rats were purchased from Taconic (Germantown, NY). Rats were housed in a temperature-controlled room (22–24 °C) with a 12-h light-to-dark cycle and allowed to consume water and a nonpurified rodent diet (5001 Lab Diet; Purina Mills, Richmond, IN) ad libitum. After the female rats became pregnant, they were separated from the males and monitored until the pups were born. Age at birth was considered day 0. The pups were kept with their dams until they were used in experiments (10 or 20–22 d old). All procedures conducted in this study were approved by the Institutional Animal Care and Use Committee, University of Medicine and Dentistry of New Jersey, New Jersey Medical School.

Experimental design

Intestinal perfusions were performed on 4, 5, or 6 rats at a time, 1 rat per perfusion solution with the number of perfusion solutions depending on the experiment (16). Perfusions were repeated for at least 4 sets of experiment ($n = 4$ or 5; see figure legends). For each replicate, 2 pups served as control and systematically received high-fructose (HF) or high-glucose (HG) solution at 100 mmol/L sugar in modified Krebs Ringer bicarbonate solution (78 mmol/L NaCl, 4.7 mmol/L KCl, 2.5 mmol/L CaCl$_2$ · 5H$_2$O, 1.2 mmol/L MgSO$_4$, 19 mmol/L NaHCO$_3$, 1.2 mmol/L KH$_2$PO$_4$). These sugar concentrations are physiologic; although lower concentrations can stimulate transporter synthesis, we intended to maximize the effect on GLUT5 and NaPi-2b. Previous work indicated postprandial, nighttime luminal glucose concentrations when adult rats consume 65% glucose or sucrose pellets to exceed 100 mmol/L (17). Daytime glucose concentrations are much lower (10 mmol/L), but in weaning rats, still partly consuming mother's milk and also feeding on 65% fructose pellets, mean daytime luminal fructose concentration already reached 26 mmol/L (16).

The effect of non- or partially metabolizable glucose analogs was tested by perfusing the intestine with 2-deoxy-D-glucose (2dG), α-methyl-D-glucose (amG), or 3-O-methyl glucose (3OmG), in addition to the HF and HG perfusions. For the experiment on the potential role of SGLT1 (intestinal sodium-glucose cotransporter type 1) in regulating NaPi-2b, pups received fructose, glucose, or 3OmG solutions along with phlorizin, a glucose uptake inhibitor. The effective (inhibitory to SGLT1) concentration of phlorizin (1 μmol/L) was determined previously by us (18). For metabolic inhibitors, sodium vanadate or sodium tungstate were used to inhibit G6Pase activity, AICAR (5-aminoimidazole-4-carboxamide-1-β-D-ribofuranoside) to activate AMPK activity, or C75 (3-carboxy-4-octyl-2-methylenebutyrolactone trans-4-carboxy-5-octyl-3-methylenebutyrolactone) to inhibit fatty acid synthase (FAS) activity. A series of bioassays were performed to determine the optimal concentration of AICAR perfusion. After testing 0, 23, 232, and 2320 μmol/L, we found that 232 μmol/L was the most effective in modulating nutrient transport. This concentration is also similar to those used for rat perfusions in vivo (19). The concentration of C75 used (37 μmol/L) was chosen on the basis of previous work in several laboratories (20, 21). The chosen concentration of vanadate and tungstate (2 mmol/L) was based on our previous work that tested several concentrations; this perfused concentration was shown to be optimal in inhibiting G6Pase activity in 20-d-old pup intestine (22). None of the chosen concentrations had an effect on mortality rate during perfusion of any of these pharmaceutical agents.

Fructose, proline, and phosphate uptake measurements

Rat intestines were perfused following the method of Jiang et al (13) and modified by Cui et al (14) in which we showed that 4 h of fructose perfusion is sufficient duration for enhancing GLUT5 mRNA and protein abundance and activity. During perfusion, rat pups were kept under continuous anesthesia, and body and perfusion solution temperatures were maintained at 37 °C. After 4 h of perfusion (30 mL/min at 37 °C), 10 cm (distal to the stomach) of proximal intestine and 10 cm (proximal to the ileocecal valve) of distal intestine were removed, and the middle intestine (≈10 cm) was placed in ice-cold Ringer solution. Of the remaining mid intestine, the proximal half was used as everted intestinal sleeves for measuring sugar, proline, and Pi uptake rates in vitro, and the distal half was quickly frozen in liquid nitrogen and then stored at −80 °C for subsequent measurements of transporter protein and mRNA concentrations. This procedure was followed for all perfusions. Because the pups were of similar body weights, had similar intestinal lengths, and were usually littermates, differences in uptake rates or expression could not be due to regional differences. When using older rats or younger pups to study developmental effects, 33% of the proximal and 33% of the distal intestines were removed, and the remainder was processed as above.

After perfusion, intestines were taken out, and everted sleeves were isolated for measurements of fructose, proline, and Pi uptake rates following the in vitro technique of Karasov and Diamond and modified by us (14). Briefly, uptake rates were measured in sleeves incubated at 37 °C in an oxygenated, stirred (1200 rpm) solution. Fructose, proline, and Pi uptake rates were determined at concentrations yielding near maximum velocity

(V_{max}) rates, so that any change in uptake will be due mainly to a change in V_{max} (23). For each rat, 2 sleeves were used for measuring uptake rates of each tested solute. The average was calculated to represent the fructose, proline, or Pi absorption in that rat.

Specific parameters used for Pi uptakes were determined by time course and dose-response studies. To determine the physiologic luminal concentration of Pi, intestinal chyme from fed pups was collected into an ice-cold container, and then measured as previously described (24). This Pi concentration was then chosen for the incubation medium in a time course study carried out between 0 and 20 min. The time of 2 min (within the initial rectilinear part of the time course) was chosen as the incubation time for the measurements of Pi uptake compared with concentration, ranging from 0 to 5 mmol/L Pi following earlier work from our laboratory (24).

Gene expression by real-time polymerase chain reaction

Total RNA was extracted; DNase was treated and reverse transcribed following the method described by Kirchner et al (22). Briefly, quantitative polymerase chain reaction (PCR) analyses for GLUT5, L-proline transporter (SIT1; sodium-dependent imino transporter 1), and NaPi-2b were performed on 10 μL of the reverse transcription (RT) reaction mixture with the use of the Brilliant SYBR Green QPCR Master Mix (Stratagene, La Jolla, CA). The total volume of the PCR reaction was 25 μL, containing 100 nmol/L of primers chosen with the PRIMER3 TOOL (http://frodo.wi.mit.edu/cgi-bin/primer3/primer3_www.cgi) (**Table 1**).

Serial dilutions of cDNAs generated from selected samples that expressed target genes at a suitable concentration were used to generate a standard curve for each target gene and the validated reference gene transcript [mRNA concentrations of the housekeeping gene elongation factor 1α (EF1α) was found independent of sugar perfused through the intestine and of developmental stage of the rat]. The standard curves were then used to determine expression values (expressed as arbitrary units of cDNA template) for each target gene after RT-PCR analysis of each sample in duplicates. Relative quantification of the target gene transcript (GLUT5, SIT1, or NaPi-2b) in comparison with EF1α expression in the same sample was made following the Pfaffl method (25).

Western blot

Brush border membrane vesicles (BBMVs) were prepared from intestinal mucosa scrapes as previously described (26). Because small neonatal intestines were used and a large amount of mucosal scrapes was required, material was pooled from different experiments. In addition, membranes from a past study were reprobed (26). Total protein (40 μg) from BBMVs or cytosol homogenate was mixed in 2× Laemmli sample buffer and run on a 10% sodium dodecyl sulfate–polyacrylamide gel electrophoresis with the use of a Mini-PROTEAN II cell (Bio-Rad Laboratories, Carlsbad, CA) for 2 h. The proteins were transferred onto a nitrocellulose membrane (Amersham Biosciences, Piscataway. NJ). Once the blots were prepared, the membrane was blocked with 5% nonfat milk in Tris-buffered saline-Tween 20 (TBS-T) (0.1% Tween 20, 50 mmol/L Tris-HCL, 137 mmol/L NaCl, pH 7.4) buffer for 1 h. The blots were then incubated with the primary antibody [rabbit anti-rat GLUT5, polyclonal β-tubulin (Chemicon International, Temecula, CA), or rabbit anti-rat NaPi-2b (US Biological, Swampscott, MA)] diluted 1:1000 in TBS-T buffer for 1 h. The membrane was incubated in the secondary antibody solution, in which a goat anti-rabbit biotinylated immunoglobulin G (Amplified Alkaline Phosphatase Goat Anti-Rabbit Immun-Blot Assay Kit; Bio-Rad) was diluted as 1:3000 in TBS-T for 30 min. Detection was performed by the formation of the streptavidin-biotinylated alkaline phosphatase complex according to the manufacturer's instructions. Purple precipitates were scanned, and the density of the blots was quantified with the use of a densitometric system (IS-1000 Digital Imaging System; Alpha Innotech, San Leandro, CA).

NaPi-2b immunofluorescence

Briefly, the mid intestine was fixed in 4% paraformaldehyde in phosphate-buffered saline (PBS) (pH 7.35) overnight at room temperature and then embedded in paraffin following earlier protocols (27). Heat-induced antigen retrieval was performed with the use of 0.01 mol/L sodium citrate buffer (pH 6.0). The sections were preincubated with 1% normal goat serum in PBS for 1 h, then with rabbit anti-rat NaPi-2b [1:500 in 1% bovine serum albumen in PBS] for 16 h at 4 °C, and then by goat anti-rabbit Cy3-conjugated immunoglobulin G (1:100; Chemicon International) for 1 h at room temperature. Coverslips were placed on slides with antifade mounting medium, and sections were then examined with a laser-scanning confocal microscope at ×40.

Statistical analyses

Data are presented as means ± SEMs. A 2-factor analysis of variance (ANOVA) was first used to determine the significance of the difference relative mRNA, protein abundances, and nutrient uptakes among groups with different treatments. If there was a significant difference, a Tukey's test was used to determine the particular effect that caused that difference. $P < 0.05$ was statistically significant, and different superscripts discriminate differences between groups. Statistical analysis used STATVIEW (Version 5; Abacus Concepts, Berkeley, CA). For Pi uptake

TABLE 1
Primers chosen for the quantification of target gene transcript[1]

Gene (protein)	GenBank AN	Forward primer (5'→3')	Reverse primer (5'→3')	Target size
				bp
Eef1a1 (EF1α)	NM_175838	ctccacttggtcgttttgctgt	agactgggggtggcaggtgtt	165
Slc34a1 (NaPi-2b)	NM_053380	gatcctttgcggctgtctgat	caccccaataccgatgagtgg	223
Slc2a5 (GLUT5)	NM_031741	tgcagagcaacgatggagaaa	acagcagcgtcagggtgaag	220
Slc6a20 (SIT1)	NM_133296	gtgtcggtgttgccagtgtg	tggatggacggtgagatgttg	226

[1] AN, accession number, EF1α, elongation factor 1α; NaPi-2b, sodium-phosphate cotransporter 2B; glucose transporter 5; SIT1, sodium-dependent imino transporter 1; bp, base pair.

experiments in nonperfused rat pups, the GRAPHPAD PRISM software (Version 4; GraphPad Software, San Diego, CA) was used for interpolating the experimental points, finding the best-fitting curve, resolving the total uptake curve in a saturable and a nonsaturable component, and calculating the kinetic constants from the saturable uptake curve.

RESULTS

Kinetics of phosphorus uptake and regional distribution of NaPi-2b in neonatal rat jejunum

We found that the intestinal luminal concentration of Pi in newly fed weaning rats was 4.8 ± 0.7 mmol/L. With the use of this concentration, we found that the increase in uptake rate was constant in the initial part of the curve until ≈ 2.5 min, so ≈ 2 min was chosen as the incubation time for the measurement of Pi uptake compared with concentration. The total Pi uptake compared with concentration curve was resolved into a saturable and a nonsaturable component. Kinetic constants were obtained from the saturable component: the apparent K_m, 2.0 ± 0.9 mmol/L; V_{max}, 0.32 ± 0.05 nmol/mg, and from the nonsaturable component, K_d, 0.016 ± 0.002 min^{-1}. The nonsaturable component represents $\approx 15\%$ of total uptake at 5 mmol/L. Because of unstirred layers, the apparent K_m from everted sleeves is a marked overestimate of the actual K_m (23) obtained from BBMVs [≈ 0.03–0.25 mmol/L (6)], but it may be closer to the apparent K_m in vivo. Because there can be large unstirred layers in the lumen in vivo, intestinal glucose transport for example has an in vivo K_m of ≈ 15 mmol/L, which is greater than the in vitro K_m of ≈ 3 mmol/L by everted sleeves and in vitro K_m of ≈ 0.5 mmol/L by BBMVs and oocytes (17, 28). Differences in K_m between our work in rat pups and those from BBMVs of adult intestine may also be because, in weaning animals, NaPi-2b is only partially glycosylated (29).

There is also a marked effect of intestinal region on NaPi-2b expression ($n = 7$; $P < 0.05$, Tukey's test). NaPi-2b mRNA abundance (normalized to the proximal) was greater in the middle ($640\% \pm 200\%$) than in the proximal ($100\% \pm 22\%$) and the distal ($164\% \pm 99\%$) intestines. These results differ from those of previous work with adult rats (30).

Can luminal sugar modulate NaPi-2b mRNA, protein abundances, and activities in the small intestine of 20-d-old rats?

Microarray screening for fructose-responsive genes in the small intestine of 20-d-old rats showed that the ratio of NaPi-2b mRNA concentrations with HF relative to HG was consistently low (ratio = 0.32) (31). With the use of real-time RT-PCR, we confirmed in this study that the HF-to-HG ratio (HF:HG) of intestinal NaPi-2b mRNA concentrations was indeed ≈ 0.3 (**Figure 1**A). In contrast, the fructose transporter GLUT5, which is known to be specifically up-regulated by luminal fructose, has a response that is the exact opposite of that of NaPi-2b. Western blots then determined whether the sugar effect on NaPi-2b gene expression was accompanied by a subsequent effect on its protein abundance (Figure 1B). β-Tubulin, a protein found only in the
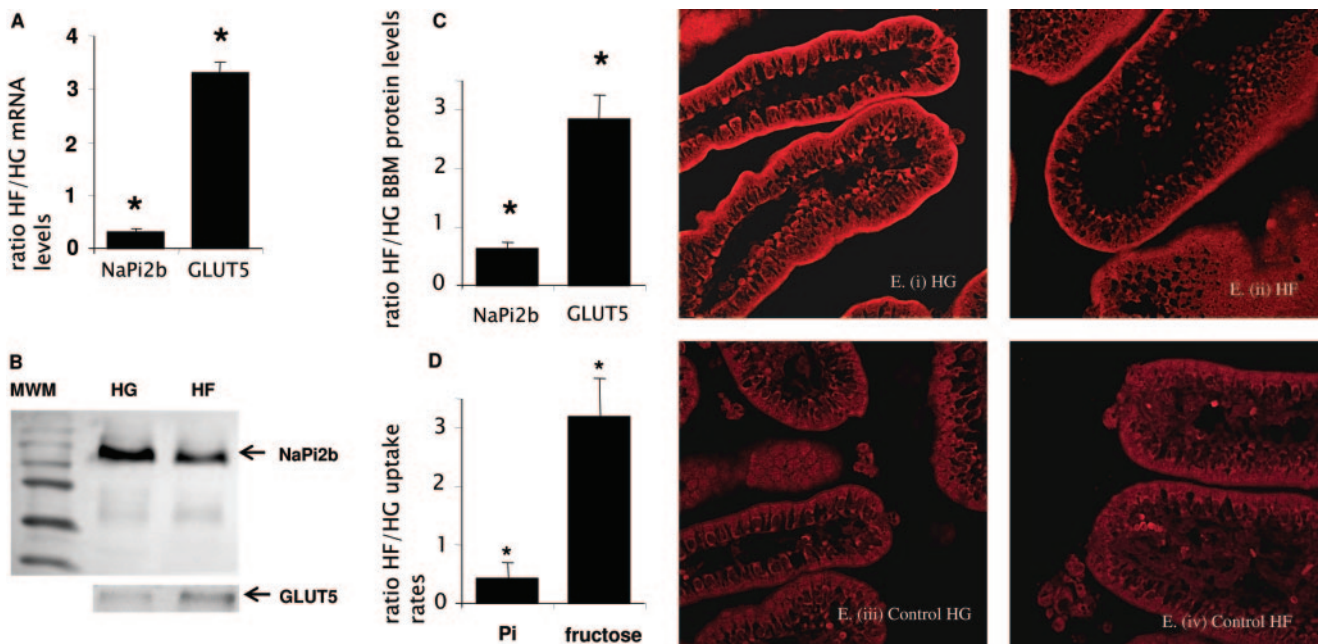
FIGURE 1. Effect of sugar perfusion on sodium-phosphate cotransporter (NaPi-2b) mRNA, protein abundance, and activity in the intestinal brush border membrane (BBM) of 20-d-old rat pups. Uptake rates and protein and mRNA concentrations were expressed as a ratio of high fructose (HF) relative to high glucose (HG). Asterisks indicate that the HF-to-HG ratio of mRNA abundance, protein concentrations, and activities was significantly different from a ratio of 1.0 ($P < 0.05$). Error bars represent means $\pm$ SEMs ($n = 4$–5). A: mRNA abundance. The ratio of NaPi-2b is $\ll 1.0$ but that of GLUT5 (glucose transporter 5) mRNA concentrations $\gg 1.0$ in HF- compared with HG-perfused intestine. B: Western blot. BBM from intestinal scrapes of 20-d-old pups perfused with HG or HF were prepared. The lane marked MWM represents molecular weight markers (NaPi-2b ≈ 100 and GLUT5 ≈ 55 kDa). C: Protein abundance. The HF-to-HG ratio of NaPi-2b is <1.0 but that of GLUT5 protein concentrations is >1.0. D: Inorganic phosphate (Pi) uptakes. The HF-to-HG ratio of Pi uptakes is significantly <1.0 and that of fructose uptake >1.0. E: Immunocytochemistry. NaPi-2b was localized to the BBM or apical membrane of enterocytes in both HG-perfused (i) and HF-perfused (ii) intestines. Controls (iii and iv), incubated in serum without anti-rat NaPi-2b, did not show any NaPi-2b in the apical membrane. Similar results were obtained from another pair of littermates whose intestines were perfused with either glucose or fructose.

cytosol and not in the apical membrane and therefore a cytosolic marker, was found in the intestinal homogenate but was not detected in the apical membrane (data not shown). NaPi-2b in the apical membrane was ≈0.5-fold in HF- compared with HG-perfused pups, whereas GLUT5 was ≈3-fold (Figure 1C). Likewise, the HF:HG of Pi uptake rates was ≈0.4-fold, whereas that of fructose uptake was 3-fold (Figure 1D). Hence, the sugar-mediated modulation of NaPi-2b gene expression discovered by microarray was confirmed by real-time PCR. Changes in NaPi-2b mRNA abundance were paralleled by similar changes in NaPi-2b protein concentrations in the apical membrane and in Pi uptake rates. NaPi-2b is localized to the apical membrane of enterocytes (Figure 1E), and immunocytochemical evidence seems to support findings of low NaPi-2b abundance in the apical membrane of HF pups (compare with Figure 1, B and C).

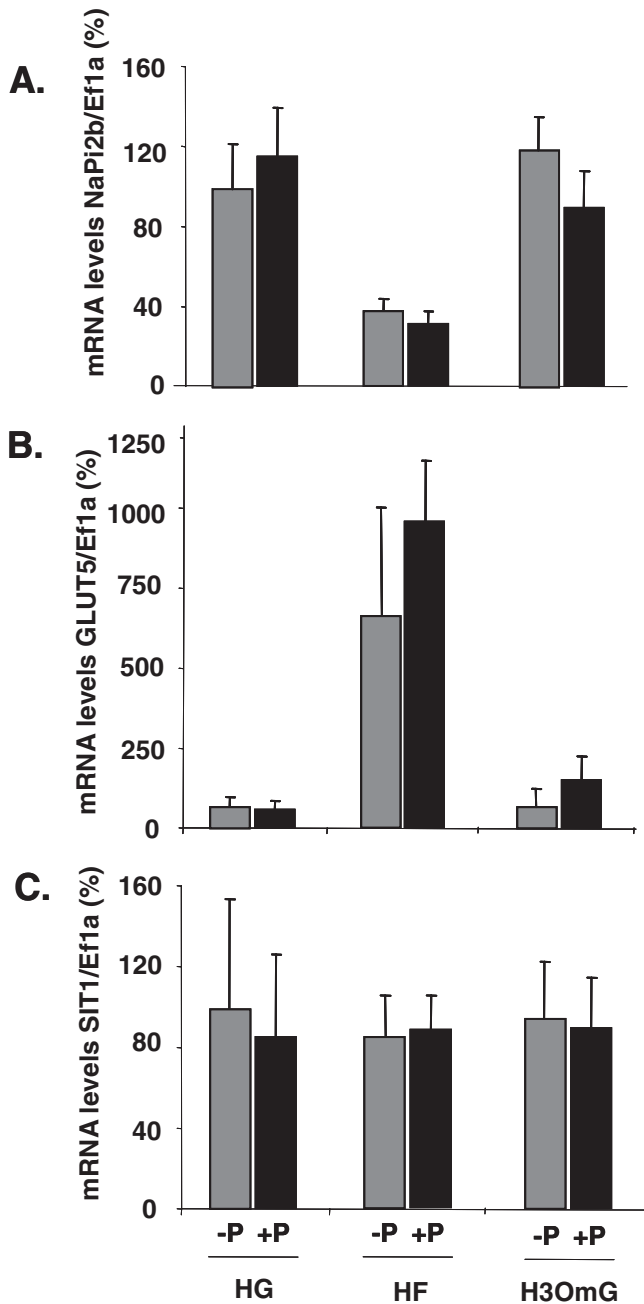### Are changes in NaPi-2b expression and activity specifically mediated by luminal glucose or fructose?

Rat intestines were perfused with 2dG and amG to determine whether intracellular glucose metabolism was required to modulate NaPi-2b gene expression and activity. Although it was remarkably clear and consistent early in our study that the HF:HG of NaPi-2b expression was small, it was difficult to establish. Therefore, we determined whether fructose decreased or glucose increased NaPi-2b. 2dG is a poorly transported sugar that is partly phosphorylated by the enterocyte (32). Although an

SGLT1 substrate, amG however cannot be catabolized in the enterocyte (33). By one-factor ANOVA, there was a significant effect ($P < 0.025$) of perfusion on NaPi-2b gene expression. NaPi-2b mRNA abundance was significantly reduced by ≈3-fold only in HF-perfused rats, whereas NaPi-2b mRNA concentrations remained high in HG-, 2dG-, and amG-perfused pups (**Figure 2**A). In contrast, expression of GLUT5 (Figure 2B) increased after perfusion with its specific substrate, fructose, but not with HG, 2dG, and amG ($P < 0.01$). Expression of SIT1, the proline transporter, was independent of perfusion solution (data not shown). Pi uptake in the HF-perfused intestine was ≈50% ($P < 0.001$, one-factor ANOVA followed by Tukey's test) that of pups given HG, high amG, or high 2dG (Figure 2C). Fructose uptake rates (Figure 2D) were in contrast up-regulated ($P < 0.01$) by ≈3-fold in HF-perfused intestines.

In a similar set of experiments, fructose, glucose, and a non-metabolizable glucose analog, 3OmG, were perfused into the intestine in the presence or absence of 1 μmol/L phlorizin that inhibits glucose and 3OmG absorption and therefore prevents these sugars from entering the intestinal cells during perfusion. By 2-factor ANOVA, there was a significant effect of perfusion solution ($P < 0.01$) but not of phlorizin ($P = 0.68$) on NaPi-2b expression. There were no interactive effects ($P = 0.50$). By Tukey's test, NaPi-2b expression was similar in both HG- and high 3OmG-perfused intestines and was greater than that in HF. After the 4-h perfusion, NaPi-2b gene expression (**Figure 3**A) in
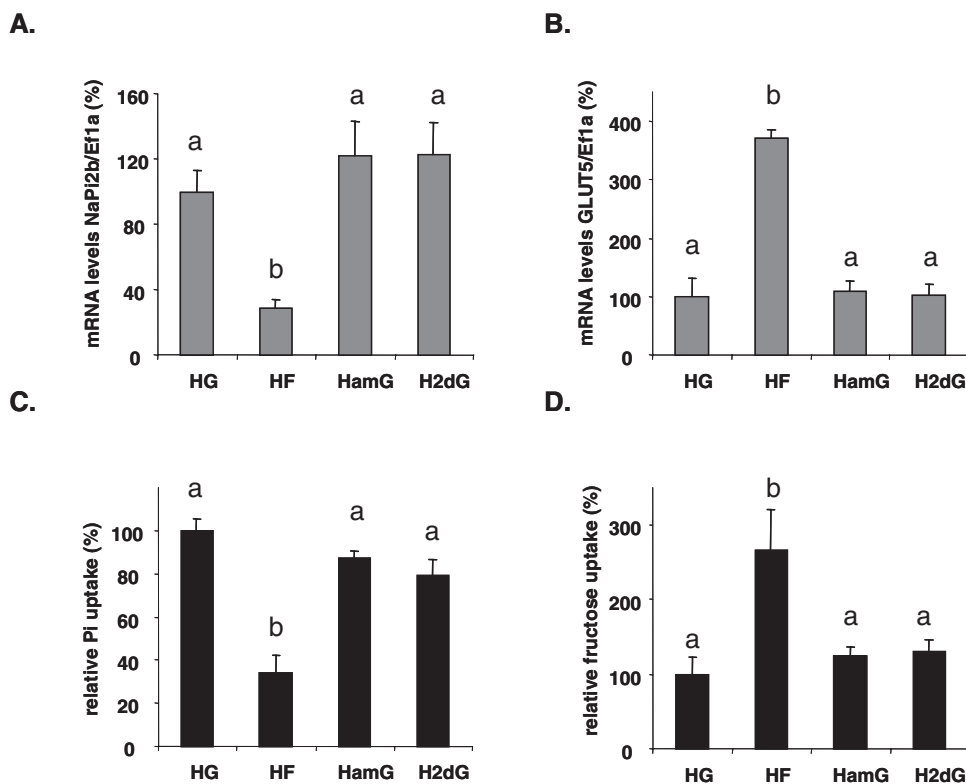
FIGURE 2. Dependence to sugar type of the luminal sugar-modulated sodium-phosphate cotransporter (NaPi-2b) expression and activity. The small intestine was perfused with 100 mmol/L glucose, fructose, or glucose analogs in Krebs Ringer Bicarbonate solution. HG, high D-glucose; HF, high D-fructose; HamG, high α-methyl-D-glucose [SGLT1 (sodium-glucose cotransporter type 1) substrate, nonmetabolized in the enterocyte]; H2dG, high 2-deoxy-glucose (poorly transported sugar that is partly phosphorylated in the cell). A: NaPi-2b mRNA abundance. B: GLUT5 (glucose transporter 5) mRNA abundance. C: Inorganic phosphate (Pi) relative uptakes. D: Fructose relative uptakes. mRNA concentrations and relative uptakes in HG-perfused pups were designated as 100% to normalize other groups to this value. Error bars represent means ± SEMs ($n = 5$). Different letters denote significant ($P < 0.05$) differences (one-factor ANOVA followed by Tukey's test). NaPi-2b mRNA concentrations and Pi uptake were down-regulated ≈3-fold in the HF-perfused relative to the HG-, HamG-, and H2dG-perfused small intestine. Ef1a, elongation factor 1α.

FIGURE 3. Dependence on glucose transport of the luminal sugar-modulated sodium-phosphate cotransporter (NaPi-2b) expression and activity in 20-d-old rat pups. The small intestine was perfused with high glucose (HG), high fructose (HF), or high 3-*O*-methyl glucose (H3OmG; sodium-glucose cotransporter type 1 transportable and non-metabolizable glucose analog) along with (+P) or without (-P) 1 μmol/L phlorizin. (A) NaPi-2b, (B) GLUT5 (glucose transporter 5), and (C) SIT1 (sodium-dependent imino transporter 1) mRNA abundance. Labels of the abscissa are the same for all 3 panels. mRNA concentrations of target genes were initially expressed relative to those of the housekeeping gene elongation factor 1α (Ef1α). The relative mRNA concentrations in HG-perfused pups were designated as 100% to normalize other groups to this value. Error bars represent means $\pm$ SEMs ($n = 5$). In the presence or absence of phlorizin, NaPi-2b expression was least in HF-perfused rats, whereas GLUT5 was greatest in HF-perfused rats(2-factor ANOVA followed by Tukey's test). SIT1 expression was independent of phlorizin or sugar treatment.

the HF− and HF+ phlorizin groups was <50% of that in the HG− and HG+ phlorizin groups, showing that glucose transport into the enterocyte is not required to modulate NaPi-2b expression. Moreover, 3OmG perfusion had no effect on NaPi-2b expression, and blocking its uptake by phlorizin also had no effect. In contrast, GLUT5 mRNA abundance (Figure 3B) increased only in the presence of fructose, and, because phlorizin does not inhibit GLUT5, its addition had no effect on GLUT5 mRNA abundance. By 2-factor ANOVA, the effect of perfusion solution on GLUT5 expression was significant ($P < 0.01$) but not that of phlorizin ($P = 0.35$); there were no interactions ($P = 0.60$). SIT1 gene expression was not affected by the modulation of glucose entry or metabolism (effect of perfusion: $P = 0.65$; effect of phlorizin: $P = 0.65$; interaction, $P = 0.91$) (Figure 3C).

After perfusion, plasma Pi concentrations were similar ($P = 0.42$) in fructose- (10.2 mg/dL or 3.3 $\pm$ 0.16 mmol/L), glucose- (9.0 mg/dL or 2.9 $\pm$ 0.36 mmol/L), and 3OmG-perfused (9.2 mg/dL or 3.0 $\pm$ 0.21 mmol/L) rats, probably because their fully functional kidneys regulated plasma Pi well within normal range [5–16 mg/dL or 1.6–5.1 mmol/L for rat plasma (34)]. In summary, fructose may be the dietary signal inhibiting NaPi-2b expression because glucose perfusion has similar effects on NaPi-2b expression as do poorly transported solutes such as 2dG, and because inhibiting glucose absorption has no effect on NaPi-2b.

Is the fructose-mediated repression of NaPi-2b expression modulated by G6Pase or AMPK?

Previous work has shown that luminal fructose markedly stimulated G6Pase expression (22) and that tungstate and vanadate perfusion inhibited G6Pase activity in both fructose- and glucose-perfused intestines (22). By 2-factor ANOVA, sugar type ($P < 0.0001$) and tungstate ($P < 0.0001$) had significant effects on NaPi-2b expression. There was also a significant interaction ($P < 0.005$). By Tukey's test, expression was less in HF than in HG and less with tungstate than without tungstate. Glucose + tungstate perfusion inhibited NaPi-2b gene expression, although not to concentrations as low as in the fructose-perfused (HF) intestines, whereas fructose + tungstate perfusion inhibited NaPi-2b expression further so that mRNA abundance was even lower than in the fructose-perfused intestine (**Figure 4**A). The proline transporter SIT1 gene expression did not vary with sugar ($P > 0.10$, 2-factor ANOVA) or tungstate ($P > 0.50$) perfusion, and there was no interaction ($P = 0.40$) (Figure 4B).

By 2-factor ANOVA, Pi uptake varied with sugar ($P < 0.001$) and tungstate ($P < 0.001$) perfusion; interaction was also highly significant ($P = 0.001$). By Tukey's test, mean uptake under HF (with and without tungstate) was less than that in HG. Likewise, mean uptake with tungstate (for both HF and HG perfused) was less than that without tungstate (Figure 4C). Proline uptake did not vary with sugar or sugar + tungstate perfusion (Figure 4D).

Consistent with the tungstate results, NaPi-2b expression varied with sugar ($P < 0.001$) and vanadate ($P < 0.001$) perfusion; interaction was also highly significant ($P < 0.001$). By Tukey's test, average expression in HF was less than in HG, whereas mean uptake with vanadate was significantly less than without (Figure 4E). Hence, when G6Pase activities were inhibited, NaPi-2b gene expression and activity decreased whether glucose or fructose was perfused along with the G6Pase inhibitor. This suggests that the effect of G6Pase on NaPi-2b is independent of the fructose effect. SIT1 gene expression (Figure 4F) was independent of
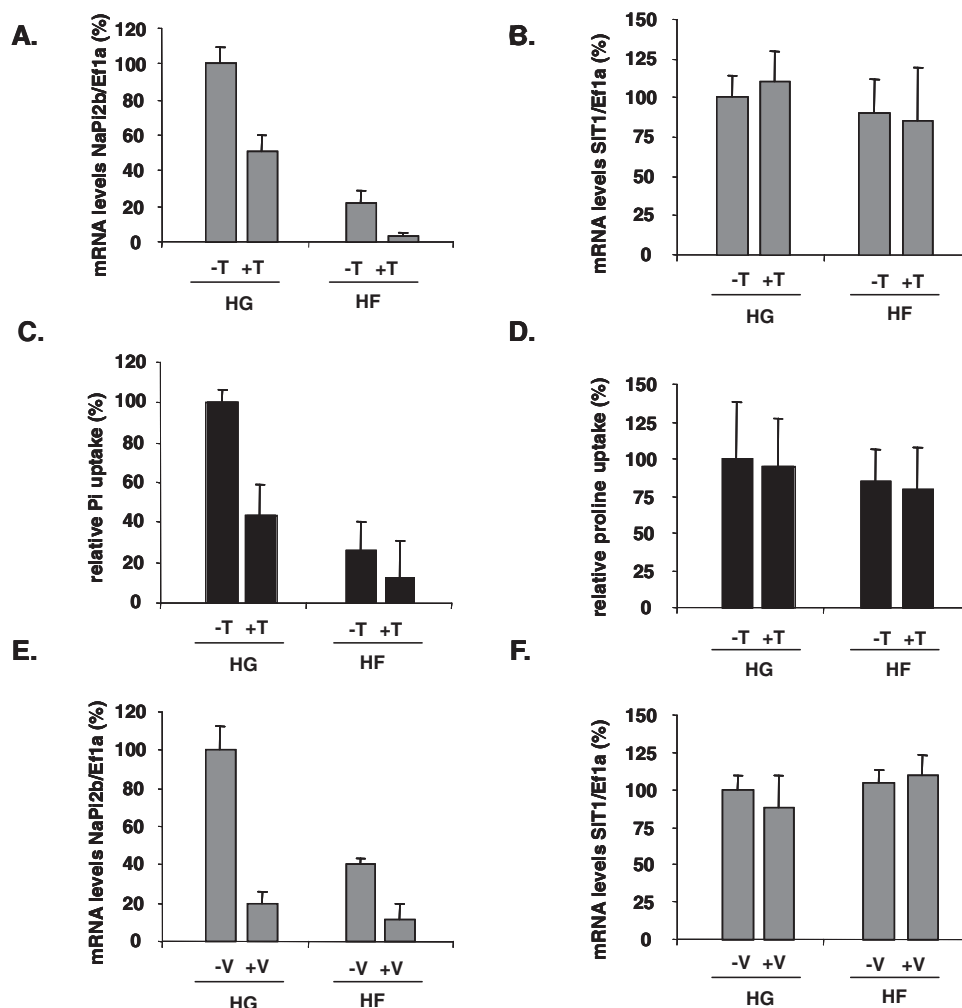
FIGURE 4. Effect of glucose-6-phosphatase (G6Pase) inhibition on fructose-induced repression of sodium-phosphate cotransporter (NaPi-2b) gene expression and of inorganic phosphate (Pi) uptake. The small intestine was perfused with high glucose (HG), high fructose (HF), or with these sugars along with a G6Pase inhibitor [vanadate (V) or tungstate (T)]. We have shown intestinal G6Pase inhibition by both vanadate and tungstate (22). L-Proline uptake and the proline transporter SIT1 (sodium-dependent imino transporter 1) were used as controls for the specificity of tungstate and vanadate effects on NaPi-2b. Effect of tungstate perfusion on (A) NaPi-2b and (B) SIT1 mRNA abundance; (C) Pi and (D) proline relative uptake. Effect of vanadate on (E) NaPi-2b and (F) SIT1 mRNA abundance. mRNA concentrations in HG-perfused pups were designated as 100% to normalize other groups to this value. Error bars represent means ± SEMs ($n = 5$). By 2-factor ANOVA, neither sugar type nor G6Pase inhibition had an effect on SIT1 gene expression. In contrast, both vanadate and tungstate significantly repressed NaPi-2b expression whether glucose or fructose was perfused along with the inhibitor. Ef1a, elongation factor 1α.

the type of sugar perfusion and of the source of G6Pase inhibition.

The effects of AMPK on NaPi-2b expression were assessed after perfusing an activator (AICAR) or an indirect inhibitor (C75) of its activity. By 2-factor ANOVA, sugar ($P < 0.001$) and AICAR ($P = 0.02$) had significant effects on NaPi-2b expression; there was no interaction ($P = 0.50$). Tukey's test showed mean expression in HF to be less than that in HG, whereas expression with AICAR was less than that without (**Figure 5**A). AICAR seemed to inhibit NaPi-2b gene expression more when fructose was perfused with the activator. SIT1 gene expression was not affected by the modulation of AMPK activities (Figure 5, B and D). By 2-factor ANOVA, sugar ($P < 0.001$) and C75 ($P = 0.01$) had significant effects on NaPi-2b expression; there was no interaction ($P = 0.40$). Consistent with the AICAR findings, NaPi-2b gene expression in glucose-perfused intestines was not affected by C75 [compare HG− and HG+ C75 (Figure 5C)]; however, it increased when FAS and AMPK were inhibited by

C75 in the fructose-perfused small intestine. Hence, activation of AMPK activities increases the inhibition of NaPi-2b by fructose, whereas inhibition of AMPK prevents the inhibition of NaPi-2b by fructose. Thus, AMPK may play an important role in the fructose-induced repression of NaPi-2b in the intestine of 20-d-old pups.

Can luminal fructose inhibit NaPi-2b expression in adults?

Because the above experiments were performed in 20-d-old rats, we determined the effect of fructose on NaPi-2b gene expression during rat development. By 2-factor ANOVA, NaPi-2b mRNA abundance varied with age ($P < 0.0005$) and perfusion solution ($P < 0.01$); interaction was significant ($P < 0.025$). By Tukey's test, mean NaPi-2b expression (in both HF and HG solutions) decreased with age, so that expression in 2-mo- and 20-d-old rats was only ≈3% and ≈20%, respectively, that in
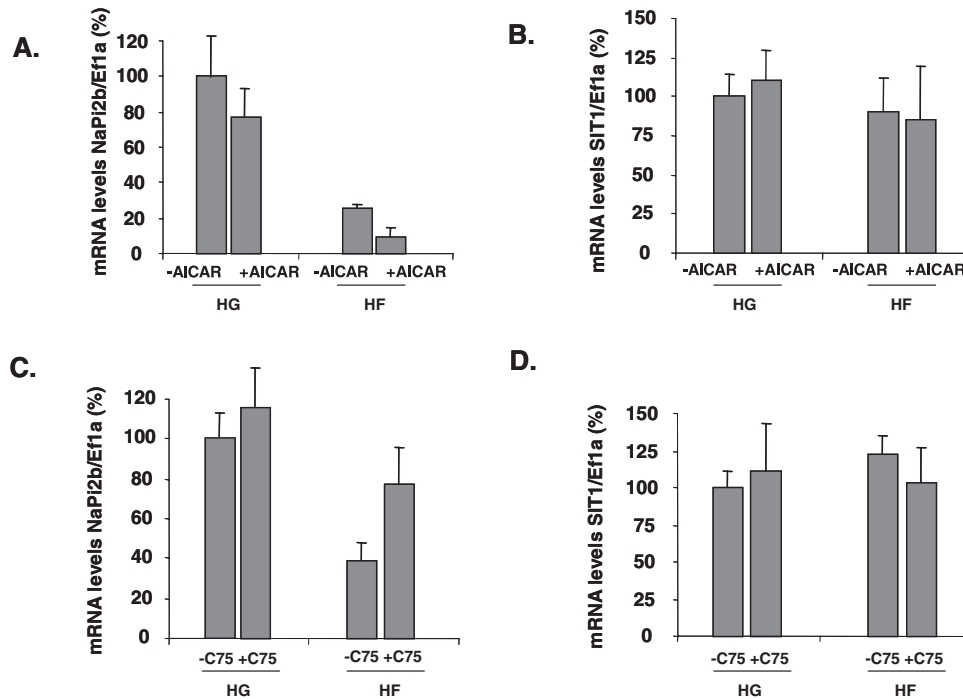
FIGURE 5. Effect of AMP kinase (AMPK) modulation on the luminal fructose-induced repression of sodium-phosphate cotransporter (NaPi-2b) gene expression and activity in 20-d-old rat pups. The small intestine was perfused with high glucose (HG), high fructose (HF), or with these sugars along with an AMPK activator [5-aminoimidazole-4-carboxamide-1-β-D-ribofuranoside (AICAR)] or fatty acid synthase–AMPK inhibitor (C75; 3-carboxy-4-octyl-2-methylenebutyrolactone *trans*-4-carboxy-5-octyl-3-methylenebutyrolactone). Effect of AICAR perfusion on (A) NaPi-2b and (B) SIT1 (sodium-dependent imino transporter 1) mRNA abundance; effect of C75 on (C) NaPi-2b and (D) SIT1 mRNA abundance. mRNA concentrations and relative uptakes in HG-perfused pups were designated as 100% to normalize other groups to this value. Error bars represent means ± SEMs ($n = 5$). By 2-factor ANOVA, neither sugar perfusion nor AMPK modulation had an effect on SIT1 gene expression. In contrast, activating AMPK enhanced the inhibition of NaPi-2b gene expression by fructose, whereas inhibiting AMPK prevented the fructose-induced repression of NaPi-2b gene expression. Ef1a, elongation factor 1α.

10-d-old pups (**Figure 6**A). No significant reduction was observed in NaPi-2b expression between 20-d- and 2-mo-old rats. Within each age group, NaPi-2b expression with fructose perfusion was only ≈40% that with glucose perfusion. Likewise, GLUT5 mRNA abundance varied with age ($P < 0.0001$, 2-factor ANOVA) and perfusion solution ($P < 0.0001$) [interaction between age and perfusion solution ($P < 0.001$)]. GLUT5 mRNA abundance increased with age, between 10 and 20 d, and then between 20 d and 2 mo (Figure 6B). Because 10-d-old rats do not express this gene, GLUT5 increased with fructose perfusion only at 20 d of age and in adults, indicating that age affects response to sugars, as suggested by the statistical interaction. Luminal fructose can inhibit intestinal NaPi-2b gene expression mainly in suckling (10 d) and weaning (20-d-old) rats, whereas its effect on GLUT5 begins in the weaning stage.

DISCUSSION

Dietary fructose inhibits NaPi-2b gene expression and activity in the neonatal rat intestine

We clearly showed that luminal fructose inhibits NaPi-2b gene expression and activity, thus showing for the first time a major interaction between 2 important constituents of the American diet, phosphate and fructose. NaPi-2b gene expression remained significantly higher in glucose- than in fructose-perfused pups when glucose transport or metabolism was prevented, suggesting that glucose does not regulate NaPi-2b expression. It also means that an increased workload for SGLT1 is not directly involved in

NaPi-2b regulation. The effect of fructose on NaPi-2b is specific because NaPi-2b expression and Pi uptake decreased, whereas GLUT5 expression and fructose uptake increased with fructose perfusion. Moreover, it is clear from different experiments that SIT1 expression and activity are also not affected, confirming the specificity of the fructose effect on NaPi-2b.

We are currently determining the mechanisms underlying the potent inhibitory effect of fructose on NaPi-2b. Because the perfusion was done in vivo, it is possible that fructose would release pancreatic and gut hormones. However, fructose is known to be a poor insulin secretagogue (35). Moreover, preliminary data ($n = 2$), obtained in isolated intestinal tissues of 20-d-old pups incubated in insulin-free solutions of 100 mmol/L HF or HG for 3 h, showed that NaPi-2b mRNA abundance in the presence of fructose was only 50% compared with that in glucose (data not shown). This suggests that the mechanism by which luminal fructose modulates NaPi-2b is primarily intracellular.

### Potential role of G6Pase in the fructose-mediated repression of NaPi-2b

A genomewide search of fructose-responsive genes with microarray hybridization identified candidate genes and potential pathways involved in the fructose-mediated regulation of NaPi-2b (31). We evaluated the role of G6Pase, because, like NaPi-2b and GLUT5, it is a fructose-responsive gene. Tungstate and vanadate are potent inhibitors of G6Pase activity in vivo (22) and can enter intestinal cells by the sulfate carrier (36, 37). Vanadium and tungsten compounds are candidates for oral therapy

A.
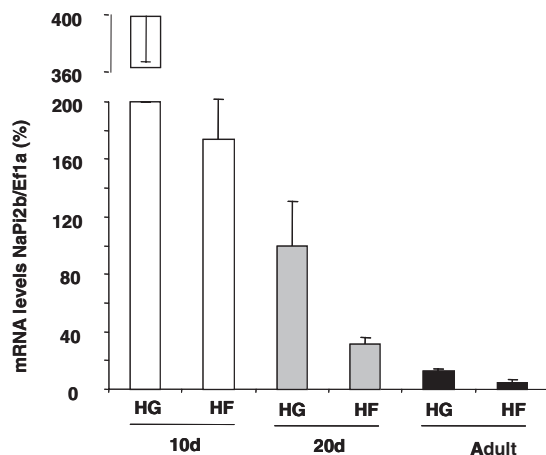
B.
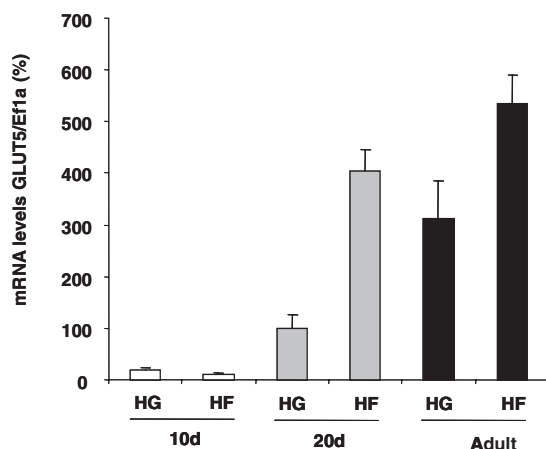
FIGURE 6. Effect of luminal fructose on sodium-phosphate cotransporter (NaPi-2b) gene expression during ontogenetic development. The small intestine of 10-d-, 20-d-, and 3-mo-old rats were perfused with high glucose (HG) or high fructose (HF). Effect of sugar perfusion and age on (A) NaPi-2b and (B) glucose transporter 5 (GLUT5) mRNA abundance. mRNA concentrations in 20-d-old HG-perfused pups were designated as 100% to normalize other groups to this value. Error bars represent means ± SEMs ($n = 5$). By 2-factor ANOVA, NaPi-2b expression decreased with age and with fructose perfusion. GLUT5 gene expression increased with age, and luminal fructose could not stimulate increases in mRNA abundance of its transporter in 10-d-old pups. Fructose stimulated GLUT5 expression in 20-d- and 2-mo-old rats. Ef1a, elongation factor 1α.

in diabetes, because they normalize not only plasma glucose but also carbohydrate and lipid metabolism by mechanisms that remain to be elucidated (38, 39). When G6Pase is inhibited, NaPi-2b expression and activity are also inhibited. Perhaps modulation of G6Pase activity alters the concentration of metabolic intermediates that regulate NaPi-2b.

Vanadate and tungstate may affect other phosphatases and even Na^+-K^+ ATPase (22) and exert their effects on Pi uptake in this manner. However, Na^+-dependent proline uptake and mRNA concentrations of the proline transporter SIT1 were not affected. Vanadate was shown to significantly reduce and delay the absorption of glucose in the small intestine of streptozotocin diabetic rats (40). However, only vanadate, but not tungstate, exerts such an effect on glucose uptakes, whereas NaPi-2b activity was affected by both inhibitors. This shows that an overall

nonspecific inhibition of sodium cotransport through the enterocyte cannot fully explain the vanadate and tungstate effects on NaPi-2b.

Potential role of AMPK in the fructose-mediated repression of NaPi-2b

Fructose is more lipogenic than is glucose (41). In rat liver, fructose feeding increases the mRNA concentrations of FAS, an important downstream enzyme in lipid synthesis (42). We hypothesized that the fructose-mediated repression of NaPi-2b mRNA concentrations and activities may be mediated by the fructose effect on FAS. We therefore inhibited FAS activities in vivo by intestinal perfusion of a known FAS inhibitor (43), C75, which also inhibits AMPK indirectly (44). NaPi-2b gene expression increased significantly only when fructose was perfused along with C75. Because C75 had no effect in glucose-perfused intestines, FAS inhibition by C75 might have prevented the fructose-induced repression of NaPi-2b. This suggests that a fructose-mediated activation of FAS occurs in the intestine and is required for NaPi-2b inhibition.

The modulation of FAS activity in the hypothalamus of mice can alter energy perception by AMPK, which functions as a physiologic energy sensor (20). AMPK is a key regulatory enzyme in the control of sugar and fatty acid metabolism in the liver and adipose tissue, able to detect energy and metabolic status, and adjust substrate flux through metabolic pathways accordingly (45). When AMPK was activated with AICAR, NaPi-2b gene expression specifically decreased in the fructose-perfused group. Thus, NaPi-2b gene expression may be linked to the metabolic state of the cell through AMPK activity.

AMPK is also known to inhibit key gluconeogenic enzymes such as G6Pase in the liver (46); hence, the inhibitory effect of AICAR on NaPi-2b is consistent with the inhibitory effect of tungstate and vanadate on NaPi-2b expression. Other potential mechanisms for the regulation of NaPi-2b involve ADP-to-ATP or NAD-to-NADH ratios. The link between NAD-NADH and NaPi-2b also warrants further investigation because systemic nicotinamide, a precursor of NAD, was shown to inhibit intestinal Pi absorption (47). When the cellular energy state is low (NAD-NADH is high), stimulation of mTOR (mammalian target of rapamycin), a protein kinase known to regulate many intestinal nutrient transporters, in turn is prevented by activation of AMPK (48). NaPi-2b was also recently shown in *Xenopus* oocytes to be stimulated by mTOR (49).

Developmental effect of luminal fructose on NaPi-2b expression in the intestine

High concentrations of NaPi-2b mRNA during ontogenesis may reflect growth-related requirements at this stage of life. High expression of NaPi-2b in the intestine and NaPi-2a in the kidney support the high bone mineralization rates essential during ontogenesis (50). In fact, the kidneys of infants and children reabsorb a large fraction of the filtered Pi by NaPi-2a (51). Because patients with ESRD have no functional kidneys, NaPi-2a no longer has a role in Pi homeostasis, and NaPi-2b becomes the only transport system that can be manipulated to modulate phosphatemia.

Per capita fructose consumption has increased by 2100% in the past century (52), and fructose is now projected to supply ≤10% of caloric intake by many Americans (11). After calcium, Pi is the

second most common micronutrient and is found in almost all foods, particularly proteins (53). Our findings show a clear interaction during the absorptive process between these 2 important nutrients, whereby fructose may negatively affect Pi absorption. If shown to lower serum Pi, consumption of fructose can also have dramatic implications for Pi metabolism and hyperphosphatemia in renal failure because even slight reductions in serum Pi concentrations result in marked decreases in mortality risk (54) for the estimated 410,000 patients with ESRD.

The options for alterations in the diets of patients with ESRD are tragically limited. Protein amounts cannot increase because of potential hyperphosphatemia and uremia, and they cannot decrease because of risks of malnutrition. Nonnutritive fiber amounts cannot increase because caloric intake must be optimal during ESRD. Hence, experimental manipulation of diets can only choose from the lesser evil of the remaining choices. Dietary fructose can isocalorically replace glucose, but it can lead to hyperlipidemia (10). Providing this option to patients with ESRD with cardiovascular problems may be counterintuitive, but, in reality, the worse option may be hyperphosphatemia because it rapidly leads to cardiovascular calcification and exacerbates or initiates the onset of cardiovascular problems (5).

REFERENCES

1. Murer H, Hernando N, Forster L, Biber J. Molecular mechanisms in proximal tubular and small intestinal phosphate reabsorption (plenary lecture). Mol Membr Biol 2001;18:3–11.

2. Saito H, Kusano K, Kinosaki M, et al. Human fibroblast growth factor-23 mutants suppress Na+-dependent phosphate co-transport activity and 1alpha,25-dihydroxyvitamin D3 production. J Biol Chem 2003;278:2206–11.

3. Capuano P, Radanovic T, Wagner CA, et al. Intestinal and renal adaptation to a low-Pi diet of type II NaPi cotransporters in vitamin D receptor- and 1alphaOHase-deficient mice. Am J Physiol Cell Physiol 2005;288:C429–34.

4. Mobjerg N, Werner A, Hansen SM, Novak I. Physiological and molecular mechanisms of inorganic phosphate handling in the toad *Bufo bufo*. Pflugers Arch 2007;454:101–13.

5. Qunibi WY. Consequences of hyperphosphatemia in patients with end-stage renal disease (ESRD). Kidney Int Suppl 2004;(90):S8–12.

6. Werner A, Kinne RK. Evolution of the Na-P(i) cotransport systems. Am J Physiol Regul Integr Comp Physiol 2001;280:R301–12.

7. Radanovic T, Wagner CA, Murer H, Biber J. Regulation of intestinal phosphate transport. I. Segmental expression and adaptation to low-P (i) diet of the type IIb Na(+)-P (i) cotransporter in mouse small intestine. Am J Physiol Gastrointest Liver Physiol 2005;288:G496–500.

8. Katai K, Tanaka H, Tatsumi S, et al. Nicotinamide inhibits sodium-dependent phosphate cotransport activity in rat small intestine. Nephrol Dial Transplant 1999;14:1195–201.

9. Xu H, Uno JK, Inouye M, et al. Regulation of intestinal NaPi-IIb cotransporter gene expression by estrogen. Am J Physiol Gastrointest Liver Physiol 2003;285:G1317–24.

10. Bray GA, Nielsen SJ, Popkin BM. Consumption of high-fructose corn syrup in beverages may play a role in the epidemic of obesity. Am J Clin Nutr 2004;79:537–43.

11. Park YK, Yetley EA. Intakes and food sources of fructose in the United States. Am J Clin Nutr 1993;58(suppl):737S–47S.

12. Ferraris RP, Diamond J. Regulation of intestinal sugar transport. Physiol Rev 1997;77:257–302.

13. Jiang L, David ES, Espina N, Ferraris RP. GLUT-5 expression in neonatal rats: crypt-villus location and age-dependent regulation. Am J Physiol Gastrointest Liver Physiol 2001;281:G666–74.

14. Cui XL, Ananian C, Perez E, Strenger A, Beuve AV, Ferraris RP. Cyclic AMP stimulates fructose transport in neonatal rat small intestine. J Nutr 2004;134:1697–703.

15. Murer H, Biber J. Renal tubular phosphate transport. In: Seldin DW, Giebisch G, eds. The kidney: physiology and pathophysiology. 2nd ed. New York, NY: Raven Press, 1992;2481–509.

16. Jiang L, Ferraris RP. Developmental reprogramming of rat GLUT-5 requires de novo mRNA and protein synthesis. Am J Physiol Gastrointest Liver Physiol 2001;280:G113–20.

17. Ferraris RP, Yasharpour S, Lloyd KC, Mirzayan R, Diamond JM. Luminal glucose concentrations in the gut under normal conditions. Am J Physiol 1990;259:G822–37.

18. Ferraris RP, Diamond JM. Use of phlorizin binding to demonstrate induction of intestinal glucose transporters. J Membr Biol 1986;94:77–82.

19. Longnus SL, Wambolt RB, Parsons HL, Brownsey RW, Allard MF. 5-Aminoimidazole-4-carboxamide 1-beta -D-ribofuranoside (AICAR) stimulates myocardial glycogenolysis by allosteric mechanisms. Am J Physiol Regul Integr Comp Physiol 2003;284:R936–44.

20. Kim EK, Miller I, Aja S, et al. C75, a fatty acid synthase inhibitor, reduces food intake via hypothalamic AMP-activated protein kinase. J Biol Chem 2004;279:19970–6.

21. Rendina AR, Cheng D. Characterization of the inactivation of rat fatty acid synthase by C75: inhibition of partial reactions and protection by substrates. Biochem J 2005;388:895–903.

22. Kirchner S, Kwon E, Muduli A, Cerqueira C, Cui XL, Ferraris RP. Vanadate but not tungstate prevents the fructose-induced increase in GLUT5 expression and fructose uptake by neonatal rat intestine. J Nutr 2006;136:2308–13.

23. Karasov WH, Diamond JM. A simple method for measuring intestinal solute uptake in vitro. J Comp Physiol 1983;152:105–16.

24. Sugiura SH, Ferraris RP. Contributions of different NaPi cotransporter isoforms to dietary regulation of P transport in the pyloric caeca and intestine of rainbow trout. J Exp Biol 2004;207:2055–64.

25. Pfaffl MW. A new mathematical model for relative quantification in real-time RT-PCR. Nucleic Acid Res 2001;29:e45.

26. Cui XL, Schlesier AM, Fisher EL, Cerqueira C, Ferraris RP. Fructose-induced increases in neonatal rat intestinal fructose transport involve the PI3-kinase/Akt signaling pathway. Am J Physiol Gastrointest Liver Physiol 2005;288:G1310–20.

27. Jiang L, Lawsky H, Coloso RM, Dudley MA, Ferraris RP. Intestinal perfusion induces rapid activation of immediate-early genes in weaning rats. Am J Physiol Regul Integr Comp Physiol 2001;281:R1274–82.

28. Wright EM, Martin MG, Turk E. Intestinal absorption in health and disease–sugars. Best Pract Res Clin Gastroenterol 2003;17:943–56.

29. Arima K, Hines ER, Kiela PR, Drees JB, Collins JF, Ghishan FK. Glucocorticoid regulation and glycosylation of mouse intestinal type IIb Na-P (i) cotransporter during ontogeny. Am J Physiol Gastrointest Liver Physiol 2002;283:G426–34.

30. Marks J, Srai SK, Biber J, Murer H, Unwin RJ, Debnam ES. Intestinal phosphate absorption and the effect of vitamin D: a comparison of rats with mice. Exp Physiol 2006;91:531–7.

31. Cui XL, Soteropoulos P, Tolias P, Ferraris RP. Fructose-responsive genes in the small intestine of neonatal rats. Physiol Genomics 2004;18: 206–17.

32. Csaky TZ. Membrane-transport of sugars in diabetes mellitus. Prog Clin Biol Res 1988;258:37–42.

33. Lostao MP, Berjon A, Barber A, Ponz F. On the multiplicity of glucose analogues transport systems in rat intestine. Rev Esp Fisiol 1991;47: 209–16.

34. Sharp PE, La Regina MC. The laboratory rat. New York, NY: CRC Press, 1998.

35. Daly M. Sugars, insulin sensitivity, and the postprandial state. Am J Clin Nutr 2003;78(suppl):865S–72S.

36. Cardin CJ, Mason J. Molybdate and tungstate transfer by rat ileum. Competitive inhibition by sulphate. Biochim Biophys Acta 1976;455: 937–46.

37. Wiegmann TB, Day HD, Patak RV. Intestinal absorption and secretion of radioactive vanadium (48VO3-) in rats and effect of Al(OH)3. J Toxicol Environ Health 1982;10:233–45.

38. Barbera A, Rodriguez-Gil JE, Guinovart JJ. Insulin-like actions of tungstate in diabetic rats. Normalization of hepatic glucose metabolism. J Biol Chem 1994;269:20047–53.

39. Goldwaser I, Gefel D, Gershonov E, Fridkin M, Shechter Y. Insulin-like effects of vanadium: basic and clinical implications. J Inorg Biochem 2000;80:21–5.

40. Ai J, Du J, Wang N, Du ZM, Yang BF. Inhibition of small-intestinal sugar absorption mediated by sodium orthovanadate Na3VO4 in rats and its mechanisms. World J Gastroenterol 2004;10:3612–5.

41. Basciano H, Federico L, Adeli K. Fructose, insulin resistance, and metabolic dyslipidemia. Nutr Metab (Lond) 2005;2:5.

42. Katsurada A, Iritani N, Fukuda H, et al. Effects of nutrients and hormones on transcriptional and post-transcriptional regulation of fatty acid synthase in rat liver. Eur J Biochem 1990;190:427–33.

43. Thupari JN, Landree LE, Ronnett GV, Kuhajda FP. C75 increases peripheral energy utilization and fatty acid oxidation in diet-induced obesity. Proc Natl Acad Sci U S A 2002;99:9498–502.

44. Ramamurthy S, Ronnett GV. Developing a head for energy sensing: AMP-activated protein kinase as a multifunctional metabolic sensor in the brain. J Physiol 2006;574:85–93.

45. Rutter GA, Da Silva Xavier G, Leclerc I. Roles of 5'-AMP-activated protein kinase (AMPK) in mammalian glucose homoeostasis. Biochem J 2003;375:1–16.

46. Hardie DG, Hawley SA, Scott JW. AMP-activated protein kinase–development of the energy sensor concept. J Physiol 2006;574:7–15.

47. Katai K, Miyamoto K, Kishida S, et al. Regulation of intestinal Na+-dependent phosphate co-transporters by a low-phosphate diet and 1,25-dihydroxyvitamin D3. Biochem J 1999;343:705–12.

48. Meijer AJ. Amino acids as regulators and components of nonproteinogenic pathways. J Nutr 2003;133(suppl):2057S–62S.

49. Shojaiefard M, Lang F. Stimulation of the intestinal phosphate transporter SLC34A2 by the protein kinase mTOR. Biochem Biophys Res Commun 2006;345:1611–4.

50. Huber K, Roesler U, Muscher A, et al. Ontogenesis of epithelial phosphate transport systems in goats. Am J Physiol Regul Integr Comp Physiol 2003;284:R413–21.

51. Spitzer A, Barac-Nieto M. Ontogeny of renal phosphate transport and the process of growth. Pediatr Nephrol 2001;16:763–71.

52. Gross LS, Li L, Ford ES, Liu S. Increased consumption of refined carbohydrates and the epidemic of type 2 diabetes in the United States: an ecologic assessment. Am J Clin Nutr 2004;79:774–9.

53. Uribarri J, Calvo MS. Hidden sources of phosphorus in the typical American diet: does it matter in nephrology? Semin Dial 2003;16:186–8.

54. Brown AJ, Finch J, Slatopolsky E. Differential effects of 19-nor-1,25-dihydroxyvitamin D(2) and 1,25-dihydroxyvitamin D(3) on intestinal calcium and phosphate transport. J Lab Clin Med 2002;139:279–84.